

Journal Pre-proofs

Design of a new type of omnidirectional shear-horizontal EMAT by the use of half-ring magnets and PCB technology

Yinghong Zhang, Wenlong Liu, Nian Li, Zhenghua Qian, Bin Wang, Dianzi Liu, Xiangyu Li

PII: S0041-624X(21)00099-8
DOI: <https://doi.org/10.1016/j.ultras.2021.106465>
Reference: ULTRAS 106465

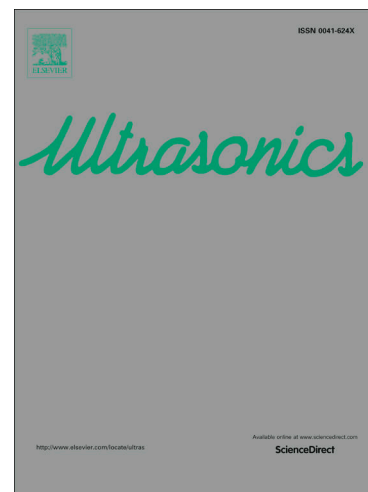
To appear in: *Ultrasonics*

Received Date: 26 September 2020
Revised Date: 21 April 2021
Accepted Date: 6 May 2021

Please cite this article as: Y. Zhang, W. Liu, N. Li, Z. Qian, B. Wang, D. Liu, X. Li, Design of a new type of omnidirectional shear-horizontal EMAT by the use of half-ring magnets and PCB technology, *Ultrasonics* (2021), doi: <https://doi.org/10.1016/j.ultras.2021.106465>

This is a PDF file of an article that has undergone enhancements after acceptance, such as the addition of a cover page and metadata, and formatting for readability, but it is not yet the definitive version of record. This version will undergo additional copyediting, typesetting and review before it is published in its final form, but we are providing this version to give early visibility of the article. Please note that, during the production process, errors may be discovered which could affect the content, and all legal disclaimers that apply to the journal pertain.

© 2021 Published by Elsevier B.V.



Design of a new type of omnidirectional shear-horizontal EMAT by the use of half-ring magnets and PCB technology

Yinghong Zhang^{1,2}, Wenlong Liu², Nian Li¹, Zhenghua Qian^{1,*}, Bin Wang¹, Dianzi

Liu³, Xiangyu Li⁴

¹ *State Key Laboratory of Mechanics and Control of Mechanical Structures, College of Aerospace Engineering, Nanjing University of Aeronautics and Astronautics, Nanjing 210016, China*

² *School of Mechanical and Electrical Engineering, Guilin University of Electronic Technology, Guilin 541004, China*

³ *School of Engineering, University of East Anglia, UK*

⁴ *Applied Mechanics and Structure Safety Key Laboratory of Sichuan Province, School of Mechanics and Engineering, Southwest Jiaotong University, Chengdu 610031, China*

Abstract In this paper, an electromagnetic acoustic transducer (EMAT) for generating and receiving omnidirectional shear-horizontal (OSH) wave in aluminum plate is developed. The proposed OSH-EMAT consists of a specially designed printed circuit board (PCB) coil and a pair of half-ring magnets. Vertical oriented static magnetic field and the radial alternative eddy current are applied to excite the Lorentz force along the circumferential direction. A three-dimensional finite element model has been established to simulate the distributions of the static magnetic flux, the eddy current, and the exciting process of SH wave. Further experimental results show that the proposed electromagnetic ultrasonic transducer has good consistency in the performance of omnidirectional excitation and reception. The new OSH-EMAT design has the potential for many non-destructive testing applications owing to its low cost, acceptable accuracy and convenient processing and fabrication.

Keywords Electromagnetic acoustic transducer, Shear-horizontal wave, Guided wave, Omnidirectional transducer.

1. Introduction

Nondestructive testing (NDT) and structural health monitoring (SHM) based on

ultrasonic guided waves have been widely applied in various engineering sectors to ensure structural integrity and safety and detect the evolution of damage. The main difference between NDT and SHM is that whether the sensors/probes are movable or fixed on the structure. The transducers should be carefully designed to meet the different engineering requirements. In this paper, we focus our research on the development of an omnidirectional shear-horizontal guided wave transducer used in NDT system.

Guided waves, usually referring to Lamb waves or SH waves traveling in a plate, have some great prospects specificity in defect location and quantitative reconstruction in plate-like structure [1-4] because their characteristics of long propagation distance and small attenuation [5]. At present, Lamb waves have achieved great success in the field of NDT&E. However, the complexity of dispersive property of Lamb wave brings considerable difficulties for the signal processing. Based on the knowledge of dispersion characteristics of guided waves, we have known that the lowest-order mode of SH wave is non-dispersive and its propagation speed remains constant. The relatively simple propagation property of SH wave helps reduce the difficulty of signal processing, which pushes forward the development of SH wave EMAT [6].

Transducer is the basic element in the guided-wave-based testing system, and the development of various guided wave transducers has always been a critical research issue [7-9]. As for SH wave transducer, it can be divided into unidirectional and omnidirectional ones based on the excitation direction. In some previous research, unidirectional SH wave transducers have been well studied and successfully applied [10-13]. However, less research can be found for the development of the omnidirectional SH wave transducer, which is useful in real engineering applications but difficult to be implemented. The omnidirectional SH wave transducer was first investigated by Z. Liu and H. M. Seung et al.[14-16] using the magnetostrictive patch transducer (MPT) technology. In their work, MPT was bonded to the specimen by epoxy resin, and was excited by alternating the electromagnetic field. The SH wave in the plate was generated along with the shear deformation of the fixed MPT. Since the SH wave MPT introduced in their work is not moveable when operating, this omnidirectional SH wave transducer cannot be used in NDT system. More recently, H. M. Seung et al. [17] reported an updated version of the omnidirectional SH wave transducer with the use of electromagnetic acoustic transducer (EMAT) technology. The EMATs used in their work are consisting of a pair of ring-type magnets (with opposite bias magnetic field) and a specific manual winding coil. However, when a large current is applied to the coil wound around the magnets, a strong electromagnetic field is

generated inside the magnets to weaken the bias magnetic field, thereby reducing the amplitude of the excited signal. On the other hand, the special wind manner of the coil is difficult to be accomplished automatically. These two defects makes the omnidirectional SH wave EMAT (OSH-EMAT) proposed in [17] hard to be used in practical engineering problems.

Motivated by the work in [17], in this paper, a new configuration of OSH-EMAT is proposed to promote its practical application in NDT system by using a specially designed printed circuit board (PCB) coil combined with the normal bias magnetic field to generate the required circumferential Lorentz force. Firstly, the configuration and working principle of the new OSH-EMAT are introduced in detail. Secondly, the excitation process of the omnidirectional SH wave is simulated by finite element method, and the optimal structure and also the frequency response characteristics are analyzed. Finally, the proposed OSH-EMAT is actually assembled; the exciting and receiving performance of this OSH-EMAT is carefully compared and verified.

2. Configuration and working principle of proposed OSH-EMAT

Figure 1 (a) depicts a SH wave propagating in a plate, with particles vibrating along the parallel direction of plate surface. x_1 , x_2 and x_3 consist a Cartesian coordinate system. Since the wave shape of omnidirectional SH wave is cylindrical, a cylindrical coordinate system is established, as shown in Fig. 1(b). The acoustic wave propagates along the r direction, and the particles vibrate along the θ direction which is also perpendicular to the propagation direction.

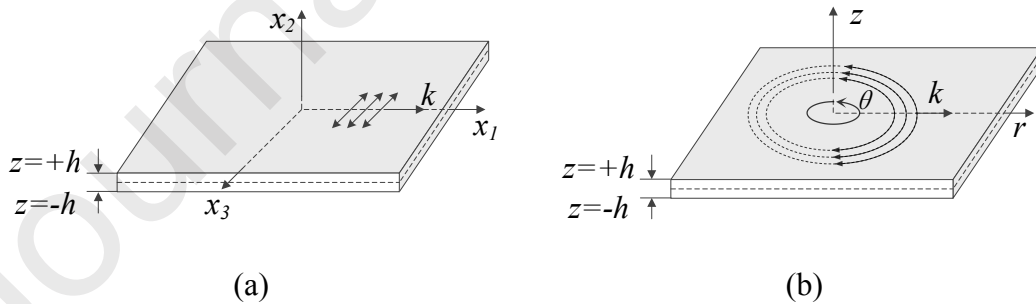


Fig. 1. Propagation model of SH wave. x_1 is the propagation direction of plane wavefront SH wave, and x_3 is the vibration direction of the particle in (a). r is the propagation direction of cylindrical SH wave, and θ is the vibration direction of the particles in (b).

To excite the omnidirectional SH wave with EMAT, it is necessary to generate a circular distributed Lorentz force in plate. The new configuration of OSH-EMAT

proposed in our work is consisting of a pair of half-ring magnets and a specially designed coil, as shown in Fig. 2. The two half-ring magnets possess opposite polarities and attract each other to form a ring. The coil is a flat fan-shaped radial multi-layered structure fabricated by printed circuit board (PCB) technology. The number of the layers of the coil structure should be an even number to form a whole assembled coil. In this paper, a double-layered coil structure is taken as an example for better understanding of the coil winding strategy.

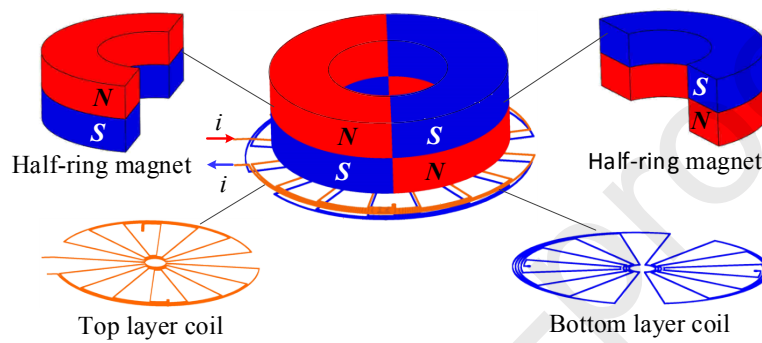


Fig. 2. Schematic of OSH-EMAT configuration. The symbol i represents current.

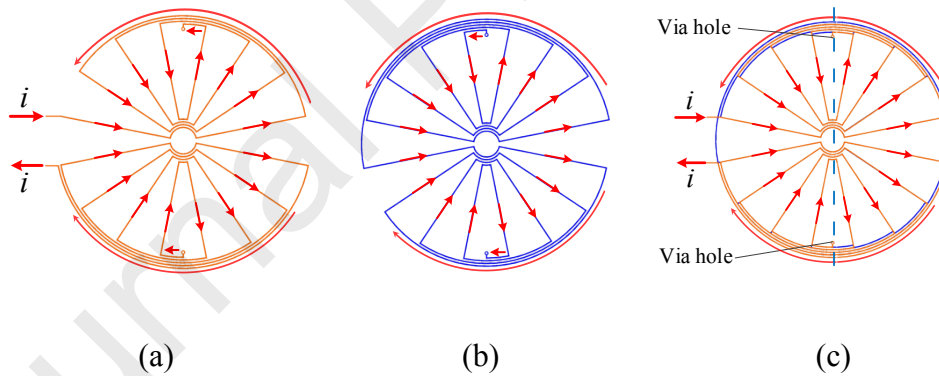


Fig. 3. Structure of the coil, (a) is the top layers, (b) is the bottom layer, and (c) is the whole assembled coil. The arrows denote the direction of current.

Fig. 3 shows the coil designing strategy. The coil consists of a top layer and a bottom layer. The top and bottom layers are connected by vias. Fig. 3(b) shows the structure of the whole coil assembled by the top layer and the bottom layer. The current in the radial wires of the left part flows toward the center, while that of the right part flows away from the center. When alternating current is applied to the coil, the eddy current induced in the specimen by the left and right coils is exactly opposite. If the two sides are provided with opposite bias magnetic fields, Lorentz force in the circumferential

direction will be generated.

Figure 4(a) shows the relative positions of the coil and the magnet in an OSH-EMAT, where the coil is placed under the two half-ring magnets. The polarity of the magnet is S at the left part, and N at the right part. The defined polarities here are only for the purpose of introducing the new configuration, which do not represent the realistic condition.

The working principle of the proposed OSH-EMAT is based on the basic rule of Lorentz force. The well-known Lorentz force expression is

$$F_L(t) = J_e(t) \times B_s \quad (1)$$

where B_s is the static bias magnetic field provided by the permanent magnet, $F_L(t)$ and $J_e(t)$ are the transient Lorentz force and eddy current density in the plate, respectively.

In the cylindrical coordinate, under the action of bias magnetic field B_s , the alternating eddy current can induce Lorentz forces perpendicular to the radial wires. The origin of this cylindrical coordinate is at the center of the EMAT, as shown in Fig. 4(b). The Lorentz forces in the circumferential can be expressed as

$$F_L(t) = J_e^r(t) e_r \times B_s^z e_z = F_L^\theta(t) e_\theta \quad (2)$$

where e_r , e_z , and e_θ represent the unit vectors in the radial, axial, and circumferential, respectively. $J_e^r(t)$ is the radial eddy current density induced in the plate, and B_s^z is the component of static magnetic flux density along z -axis. According to equation (2), the scalar expression of the circumferential Lorentz force is

$$F_L^\theta = J_e^r \times B_s^z \quad (3)$$

It can be seen from Fig. 4(b) that the direction of eddy current and bias magnetic field on the left side are exactly opposite to that on the right side in the cylindrical coordinate, which ensures the Lorentz force in left and right parts having the same circumferential direction (clockwise or anticlockwise). The alternating Lorentz force will cause in-plane shear motion vibrating along the circumferential direction, and then generate SH waves propagating along the radial direction. An omnidirectional SH wave can then be excited with this new configuration of EMAT.

3. Simulation of the proposed OSH-EMAT

3.1. Model establishment

The widely used two-dimensional simplified model cannot be used in this work because the proposed OSH-EMAT is a non-axisymmetric structure whose working

principle can only be fully described by the exact three-dimensional model. Therefore, we establish a three-dimensional model of the proposed OSH-EMAT in the finite element software COMSOL Multiphysics. To reduce computing resources, the coil structure is simplified to a series of uniformly distributed radial wires. The arc wires are removed because it does not contribute to exciting the circumferential Lorentz force. The inner diameter d of the magnet is taken to be 10mm, medium diameter d_m to be 20mm, and external diameter D to be 30mm. The lift-off distance of the magnets is 1mm. The thickness of the plate is 3mm.

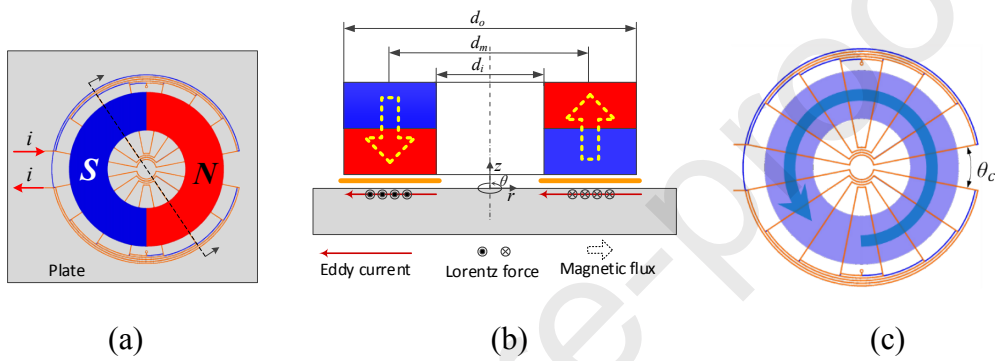


Fig. 4. Schematic diagram of the proposed OSH-EMAT, (a) is the top view, (b) is the cross-sectional view, and (c) is the circumferential Lorentz force.

To maximize the EMAT output, the center frequency of the excitation signal (or the wavelength) needs to be determined first. The excitation frequency is relating with the phase velocity C_p and the wavelength λ through

$$f = C_p / \lambda \quad (4)$$

where the phase velocity of SH mode can be calculated from the dispersion equation introduced in [18]. In some previous research [10, 19, 20], it has been revealed that in annular array type transducer, the output displacement amplitude will reach maximum when the wavelength of the transducer satisfies $\lambda = d_m$. However, this conclusion does not hold for the proposed EMAT in this paper because the distribution density of the coil is uneven along radial direction so that mutual interference waves will be generated at different radii. Therefore, further investigation is required to determine the optimal excitation frequency, which will be conducted by experiment method.

3.2. Analysis of simulation results

In the simulation model, two Magnetic Fields modules and one Solid Mechanics module are included. One Magnetic Fields module is used to calculate the static bias

magnetic field, the other is used to calculate the alternating eddy current induced in the plate. The Solid Mechanics (elastic wave) module is used to calculate the generated Lorentz force. In the following subsections, some basic characteristics of the proposed OSH-EMAT will be discussed in detail, including the static magnetic field, the induced eddy current, the Lorentz force, the excited wave shape, etc.

3.2.1 Static magnetic field

The static magnetic flux density is calculated in the “Magnetic field” module. Figure 5 shows the magnetic flux density B_z on the surface of the aluminum plate at $r = 10$ mm. We can find that the magnitude of B_z is nearly uniformly distributed along the middle circumference of the half-ring magnet, with opposite directions under the left and right magnets. The magnetic field near the seam reverses sharply, and the magnetic flux superposition at the seam is zero.

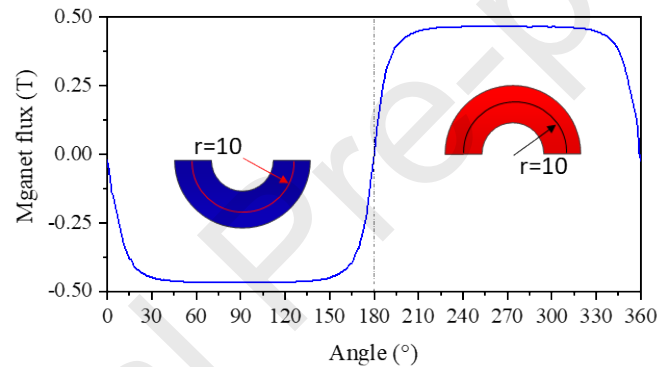


Fig. 5. Distribution of static magnetic flux density on the middle diameter of magnets.

3.2.2 Eddy current and Lorentz force

The simulation of the time-dependent electromagnetic field is performed in "Magnetic Field 2". A sinusoidal current signal modulated by the Hanning window with 5 cycles is fed to the coil. This alternating current will generate a dynamic magnetic field, which will further induce a dynamic eddy current in the skin depth of the aluminum plate. Fig. 6 shows the eddy current distribution at $t = 11.8 \mu\text{s}$. It is easy to find that the directions of the eddy current are opposite at the left and right parts. Therefore, as we expected, a circumferential Lorentz force with the same direction can be generated under the action of the basis magnetic fields and the eddy currents introduced. We can also find that the magnitude of the eddy current density takes a larger value near the center region, which is mainly arising from the uneven radial

density of the fan-shaped wires. As a result, the Lorentz force will also be unevenly distributed in the radial direction.

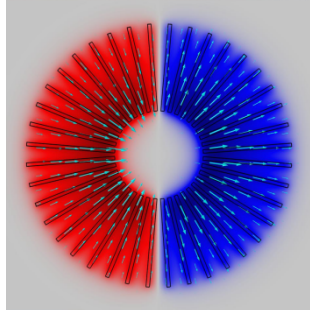


Fig. 6. Snapshot of radial eddy current density in the plate at $t=11.8 \mu\text{s}$

The simulation of the Lorentz force is performed in the "Solid Mechanics" module. Fig. 7 shows the distribution of stress in the plate at different times and also the circumferential radiation pattern. The magnitude of Lorentz force near the seam area is relatively smaller at the beginning period of the excitation process, but becomes unobvious as the time goes. It has been revealed in [21] that the guided wave field excited by EMAT can be calculated from the superposition of those excited by the suitable point or line excitation sources. As the propagation distance increases, the wave will gradually diverge and reach local equilibrium. The radiation pattern at a distance of 70mm from the transducer are shown in Figure 7(d), where we can find that the excitation amplitude at the seam area is about 18% lower than that at the middle part of the magnet. The qualitative results prove that the reduction effect of the Lorentz force caused by magnetic field reversal in the seam area is acceptable for engineering applications.

The working performance of EMAT is directly relating with its structure. Therefore, to optimize the performance of OSH-EMAT, a series of results with different θ_c are calculated and compared, which are respectively $\theta_c = 15^\circ, 11.25^\circ, 9^\circ, 7.5^\circ$. The calculation results are plotted in Fig. 8. The displacement amplitude linearly increases with the conductor angle decreases, which indicates that a denser circumferential wire can generate larger output displacement.

3.2.4 SH wave mode

Fig. 9 (a) shows the displacement distribution of the SH wave excited by the proposed OSH-EMAT. The displacement components of the particles are mainly along circumferential direction, and the particles vibrate in opposite direction with a distance of half-wavelength in radial direction. Fig. 9 (b) shows the three components of the

displacement at $r=50$ mm. The displacement component in θ direction is much larger than that in r and z direction, which means that the circumferential displacement component is dominated. Fig. 9 (c) shows the SH wave signal received at the place of 150mm away from the transmitter. The calculated group velocity is about 3061m/s, and no other unwanted modes are generated. All these features are consistent with what we have known about SH waves, which verify the capacity of generating the SH guided wave by the proposed OSH-EMAT.

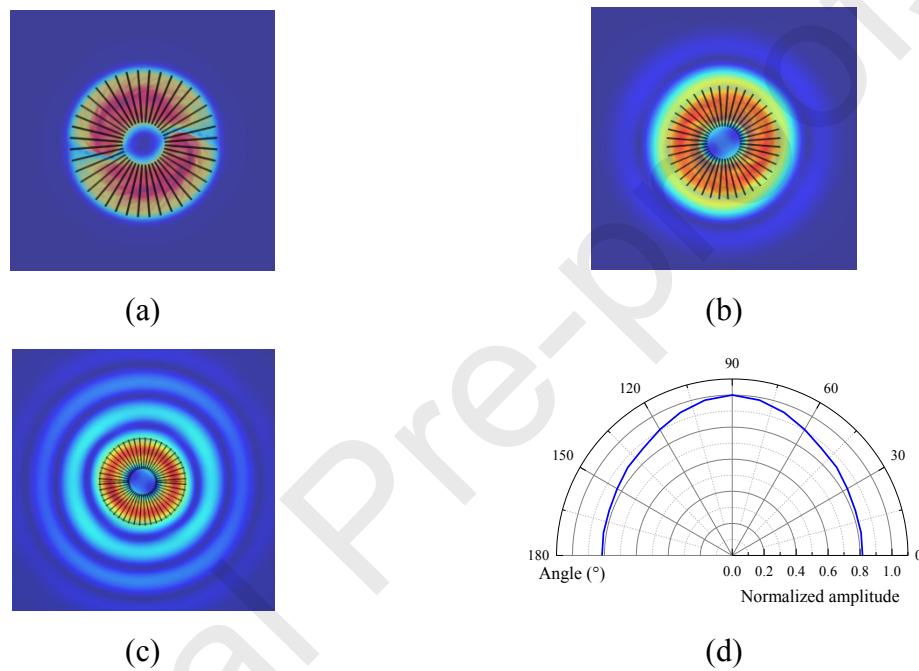


Fig. 7. Snapshots of circumferential Lorentz force in the plate at different times, (a) is at $t= 3.16 \mu\text{s}$, (b) is at $t=8.7 \mu\text{s}$, (c) is at $t=18.2 \mu\text{s}$, and (d) is the circumferential radiation pattern.

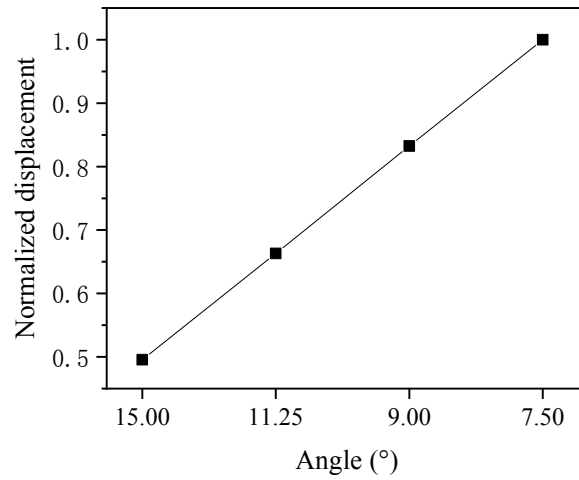


Fig. 8. Relation curve between conductor included angle and output displacement.

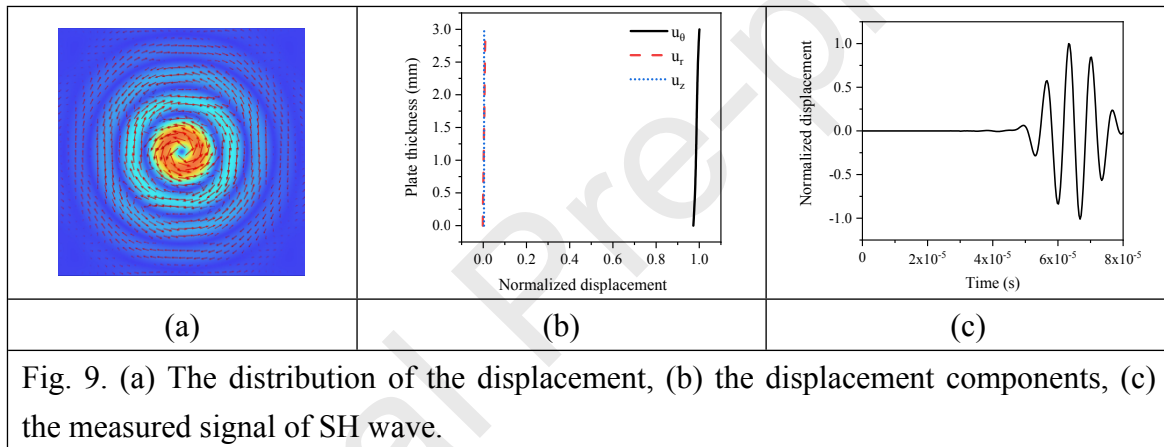


Fig. 9. (a) The distribution of the displacement, (b) the displacement components, (c) the measured signal of SH wave.

4. Experiments

In this section, the performance of the proposed OSH-EMAT is verified by experiments. The experimental setup is shown in Fig. 10, consisting of an arbitrary function signal generator, a high-power ultrasonic test system RPR-4000, a digital oscilloscope MOS2022, an impedance matching network, a pair of EMATs and an aluminum plate. The transducer and receiver are placed on an aluminum plate with the size of 1200mm×900mm×3mm. In EMAT, the coil is a double-layered structure made by PCB technology, with the thickness of each layer being 0.6mm; the half-ring magnets are obtained by cutting the ring type NdFeB magnet using the Electrical Discharge Machining (EDM) process.

When collecting signals, the function signal generator sends out an exciting signal and a synchronization trigger signal to the power amplifier and the digital oscilloscope simultaneously. After receiving the synchronization trigger signal, the high-power

amplifier opens the output channel. The oscilloscope uses the synchronous trigger signal as a reference point to the receiving signal.

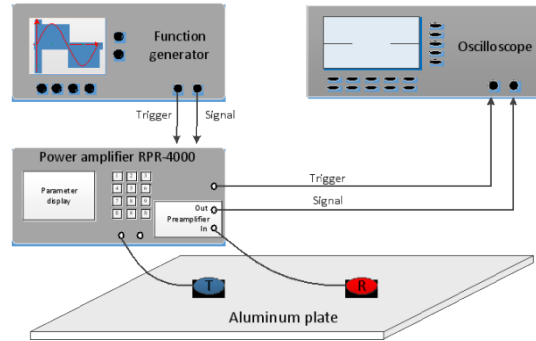


Fig. 10. Experimental setup for the SH wave transduction in a pitch-catch manner.

4.1. Generation and reception SH wave

Firstly, we need to verify whether the excited wave is SH wave. The distance between the transducer and the receiver is 600mm, and the receiver is 150mm away from the plate edge. The excitation voltage is fixed as 306V in all the experimental measurements. The frequencies of 80 kHz, 105 kHz, and 130 kHz are used for excitation, respectively. The signal amplitudes collected under these three excitation frequencies are shown in Fig. 11. With the change of frequency, there is no obvious distortion or tailing on the mode shape, only the signal amplitude slightly varies, which indicates that the excited wave is a non-dispersive wave. The signal-to-noise ratios (SNR) at these three frequencies are 26.8dB, 28.5dB and 27.7dB respectively. The group velocity of the excited wave is calculated as 3140 m/s from the figure, which is close to the theoretical group velocity of SH₀ mode guided wave. No other unwanted modes are measured in the received signals. These results indicate that the proposed OSH-EMAT can excite pure SH₀ mode guided wave, which is consistent with the simulation result.

Secondly, to verify the relationship between the conductor-included-angle and the output amplitude as shown in Fig. 8, a series of coils with 24, 32, 40 and 48 circumferential conductors are designed, which determines the conductor included angle as 15, 11.25, 9 and 7.5, respectively. In the experiment, coils with different included angles are used to excite SH waves, and a unidirectional SH wave transducer made of a racetrack-shaped coil is used for signal reception. As shown in Fig. 12, the experimental results are in good consistent with the simulation results shown in Fig. 8, which again proves that the number of coil turns is proportional to the amplitude of the output signal.

Therefore, in engineering applications, the number of conductors should be increased as much as possible to improve the output efficiency of the transducer.

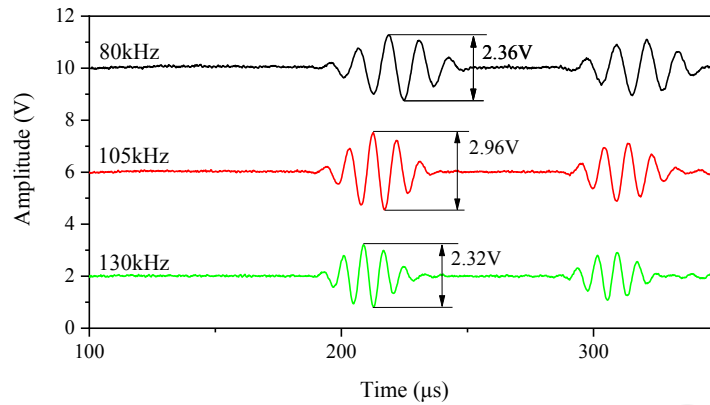


Fig. 11. EMAT output signals measured at different excitation frequencies.

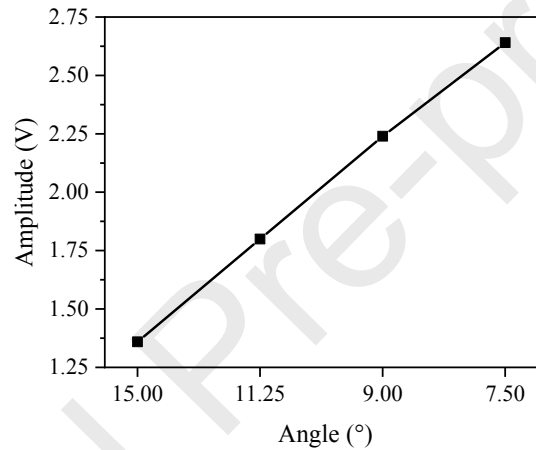


Fig. 12. Experimental results of the relationship between conductor included angle and output signal amplitude.

4.2. Investigation of transducer characteristics

4.2.1. Frequency characteristics of OSH-EMAT

The center frequency of EMAT is relating to the geometric size of the permanent magnet. In this section, four pairs of magnets with different diameters are used, and the corresponding experiment parameters and results are listed in Table 1. In all the experiment measurements, the interval of the excitation frequency is set as 5 kHz. By measuring the peak-to-peak value of the signal excited by the different excitation frequencies, the center frequency with the largest signal amplitude can then be obtained. The wavelength at each excitation frequency can be calculated according to Eq. (4). Fig. 13 shows relationship between the ratio of the wavelength to the outer diameter of magnet and the different excitation frequency. It can be observed from Fig. 13 that the signal amplitude reaches maximum when the ratio of wavelength to outer diameter is one or close to one. The center frequency of the OSH-EMAT can then be determined by

the outer diameter of the half-ring magnet with this finding.

Table 1. Parameters of the EMAT and experimental results of frequency characteristics

Case number	d (mm)	D (mm)	Sweep frequency range	Peak value frequency (kHz)	Calculated wavelength λ (mm)
1	10	30	65-135	100,105	31.4,29.9
2	20	30	65-135	95	33
3	8	25	65-165	125	25.12
4	15	25	65-165	120,125	26.2,25.1

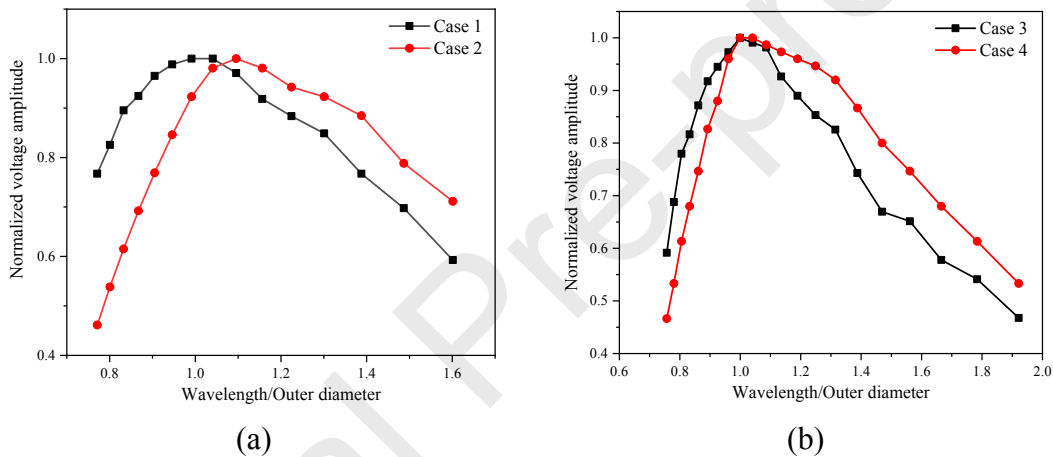


Fig. 13. The relationship between the ratio of wavelength to magnet outer diameter and signal amplitude at different frequencies. (a) The outer diameter of the magnet is 30mm. (b) The outer diameter of the magnet is 25mm.

Fig. 14 shows the output signals of EMAT with magnets of different sizes. The results show that with the same external diameter of the magnet, the signal amplitude generated by EMAT increases with the decrease of the inner diameter of the magnet. This is because the smaller the inner diameter of the magnet, the larger the volume of the magnet, so the greater the intensity of the bias magnetic field. Therefore, in practical applications, the radial thickness of the ring magnet should be as large as possible to maximize the output.

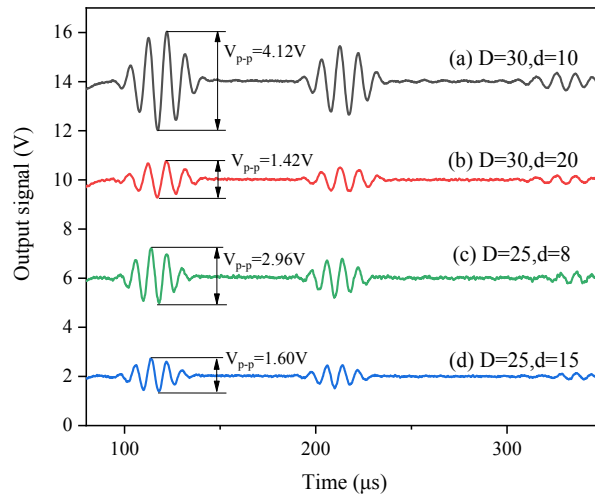


Fig. 14. The output signal of EMAT with magnets of different sizes.

4.2.2. Circumferential consistency of the proposed EMAT

In this section, the circumferential radiation pattern of the developed OSH-EMAT is tested to verify the omnidirectional performance of the proposed OSH-EMAT. For comparison, two sets of experiments are performed with the OSH-EMAT as transmitter or receiver respectively, whose experimental setups are as shown in Fig. 15. The distance between the transmitter and the receiver is 300mm. In the measurement process, first fix the transmitter and rotate the receiver to collect the signal, then fix the receiver and rotate the transmitter to excite the signal. The rotation step is 9 degrees, and the acquisition range is 0-180 degrees. By extracting the peak-to-peak values from the measured signals, the radiation patterns of the developed OSH-EMAT are obtained. The results are plotted in Fig. 15. The experimental results are in good consistent with the circumferential radiation pattern shown in Fig. 7(d). When the seam is used as a wavefront, the amplitude of the transmitted and received signals is about 20% lower than that of the center of the magnet as the wavefront, which is acceptable for engineering application. We can conclude that the performance of the proposed OSH-EMAT is almost consistent at different angle, no matter as a transmitter or receiver.



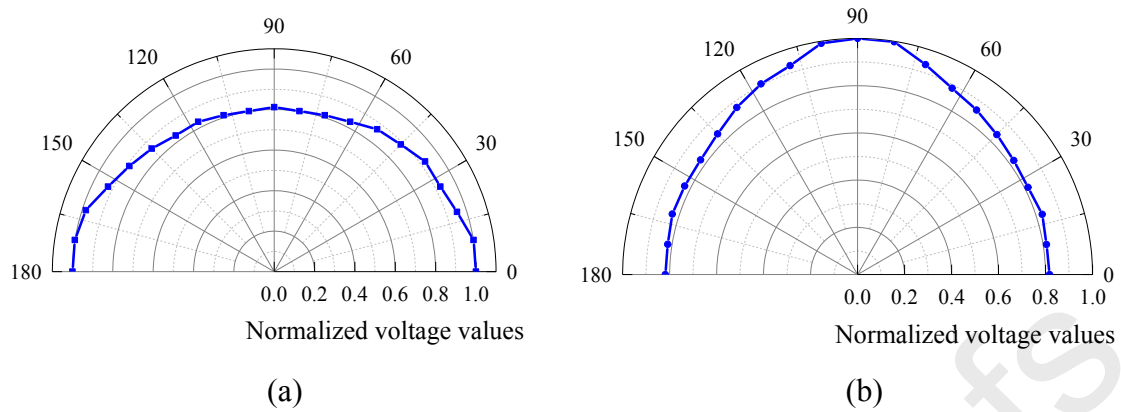


Fig. 15. Experimental setups to check the circumferential radiation patterns. (a) Fix the transmitter and use the magnets seam as the wavefront. (b) Fix the receiver and use the center of magnet as the wavefront.

5. Conclusion

In this paper, a novel configuration of Lorentz-force-based OSH-EMAT is proposed. The transducer consists of two half-ring permanent magnets with opposite polarities and a specifically designed PCB coil. Simulation results show that the output performance of the OSH-EMAT is linearly dependent with the angle between the radial lines of the coil, the smaller this angle, the larger the output amplitude is. Further verifications are carefully taken with a series of experiments. The results demonstrate that the center frequency of the OSH-EMAT is determined with the external diameter of the half-ring magnets. Additionally, comparing the amplitudes of four excitation magnetic ring with different diameters, it is concluded that increasing the radial thickness of the magnetic can increase the output amplitude of the transducer. The omnidirectional property of the proposed EMAT is finally verified. Also, it is necessary to be noticed that, since the z-direction magnetic field in the joint area of the magnet pair is slightly smaller than other positions, there will be a certain decrease of the omnidirectional performance. In practical application, this disadvantage can be resolved easily by placing the ring magnet directly in the middle of the ring area. All these results strongly prove that the proposed OSH-EMAT can be used in real engineering applications with outstanding performance.

Acknowledgements

This work was funded by the National Natural Science Foundation of China (No.

12061131013), the State Key Laboratory of Mechanics and Control of Mechanical Structures at NUAA (MCMS-E-0520K02), the Guangxi Key Laboratory of Manufacturing System and Advanced Manufacturing Technology (17-259-05-005Z), the Opening Project of Applied Mechanics and Structure Safety Key Laboratory of Sichuan Province (SZDKF-202002), and the Priority Academic Program Development of Jiangsu Higher Education Institutions (PAPD).

Author Statement

Yinghong Zhang: Writing-Original draft, Investigation, Conceptualization, Methodology.

Wenlong Liu: Experiment, Data curation, Visualization.

Nian Li: Validation, Writing- Reviewing and Editing.

Zhenghua Qian: Resources, Supervision, Project administration, Funding acquisition.

Bin Wang: Software, Validation.

Dianzi Liu: Writing- Reviewing and Editing, Methodology, Formal analysis.

Xiangyu Li: Resources, Revision.

References

- [1] Z. Wei, S.L. Huang, S. Wang, W. Zhao, Magnetostriction-Based Omni-Directional Guided Wave Transducer for High-Accuracy Tomography of Steel Plate Defects, *Ieee Sens J*, 15 (2015) 6549-6558.
- [2] N.K. Mutlib, S. Bin Baharom, A. El-Shafie, M.Z. Nuawi, Ultrasonic health monitoring in structural engineering: buildings and bridges, *Struct Control Hlth*, 23 (2016) 409-422.
- [3] W. Li, Y. Cho, Quantification and imaging of corrosion wall thinning using shear horizontal guided waves generated by magnetostrictive sensors, *Sensors and Actuators A: Physical*, 232 (2015) 251-258.
- [4] P. Belanger, P. Cawley, F. Simonetti, Guided wave diffraction tomography within the born approximation, *Ieee T Ultrason Ferr*, 57 (2010) 1405-1418.
- [5] R. Jarvis, P. Cawley, P.B. Nagy, Current deflection NDE for the inspection and monitoring of pipes, *NDT & E International*, 81 (2016) 46-59.
- [6] S. Legendre, D. Massicotte, J. Goyette, T.K. Bose, Wavelet-transform-based method of analysis for lamb-wave ultrasonic NDE signals, *Ieee T Instrum Meas*, 49 (2000) 524-530.
- [7] Y.Y. Kim, Y.E. Kwon, Review of magnetostrictive patch transducers and applications in ultrasonic nondestructive testing of waveguides, *Ultrasonics*, 62 (2015) 3-19.
- [8] Z. Liu, Y. Hu, M. Xie, B. Wu, C. He, Development of omnidirectional A 0 mode EMAT employing a concentric permanent magnet pairs with opposite polarity for plate inspection, *NDT & E International*, 94 (2018) 13-21.
- [9] W. Wright, D. Hutchins, D. Jansen, D. Schindel, Air-coupled lamb wave tomography, *Ieee T Ultrason Ferr*, 44 (1997) 53-59.

- [10] R. Ribichini, F. Cegla, P.B. Nagy, P. Cawley, Study and Comparison of Different EMAT Configurations for SH Wave Inspection, *Ieee T Ultrason Ferr*, 58 (2011) 2571-2581.
- [11] J. Parra-Raad, P. Khalili, F. Cegla, Shear waves with orthogonal polarisations for thickness measurement and crack detection using EMATs, *NDT & E International*, 111 (2020).
- [12] H.-S. Yoon, D. Jung, J.-H. Kim, Lamb wave generation and detection using piezoceramic stack transducers for structural health monitoring applications, *Smart Mater Struct*, 21 (2012) 055019.
- [13] R. Murayama, H. Hoshihara, T. Fukushige, Development of an electromagnetic acoustic transducer that can alternately drive the lamb wave and shear horizontal plate wave, *Jpn J Appl Phys* 1, 42 (2003) 3180-3183.
- [14] Z. Liu, Y. Zhang, M. Xie, A. Li, W. Bin, C. He, A direction-tunable shear horizontal mode array magnetostrictive patch transducer, *NDT & E International*, 97 (2018) 20-31.
- [15] H.M. Seung, H.W. Kim, Y.Y. Kim, Development of an omni-directional shear-horizontal wave magnetostrictive patch transducer for plates, *Ultrasonics*, 53 (2013) 1304-1308.
- [16] H.M. Seung, Y.Y. Kim, Generation of omni-directional shear-horizontal waves in a ferromagnetic plate by a magnetostrictive patch transducer, *NDT & E International*, 80 (2016) 6-14.
- [17] H.M. Seung, C.I. Park, Y.Y. Kim, An omnidirectional shear-horizontal guided wave EMAT for a metallic plate, *Ultrasonics*, 69 (2016) 58-66.
- [18] J.L. Rose, *Ultrasonic Waves in Solid Media*, Cambridge University Press, New York, 1999.
- [19] E.V. Glushkov, N.V. Glushkova, O.V. Kvasha, R. Lammering, Selective Lamb mode excitation by piezoelectric coaxial ring actuators, *Smart Mater Struct*, 19 (2010) 035018.
- [20] C.F. Vasile, R.B. Thompson, Excitation of horizontally polarized shear elastic waves by electromagnetic transducers with periodic permanent magnets, *J Appl Phys*, 50 (1979) 2583-2588.
- [21] P. Wilcox, Modeling the Excitation of Lamb and SH Waves by Point and Line Sources, 700 (2004) 206-213.

Highlights

- A new type of OSH-EMAT was designed by the use of half-ring magnets and PCB technology.
- The EMAT can generate in-plane circumferential Lorentz force in a non-contact manner.
- The number of the radial conductors is proved to be linearly relating with the output efficiency of the proposed EMAT.
- The proposed EMAT can generate and/or receive SH₀ mode guided wave with good omnidirectional performance.

Declaration of interests

The authors declare that they have no known competing financial interests or personal relationships that could have appeared to influence the work reported in this paper.

The authors declare the following financial interests/personal relationships which may be considered as potential competing interests:

Journal Pre-proofs